

# Ovarian Cellular Fibroma: Magnetic Resonance Imaging Findings With Pathological Correlation

Yuka Sano<sup>a, c</sup>, Tetsuo Maeda<sup>b</sup>, Kazuhiro Kitajima<sup>c</sup>, Takahiro Watanabe<sup>d</sup>,  
Reina Miki<sup>a</sup>, Mieko Inagaki<sup>a</sup>, Shigeki Yoshida<sup>a</sup>

## Abstract

Ovarian cellular fibromas are relatively rare and generally have a favorable prognosis. However, their recurrence can occur in cases involving rupture or adhesion. Preoperative diagnosis is crucial for determining the surgical approach and tumor retrieval methods. To date, the radiological findings of this tumor have not been well documented in the literature. We report the case of a 60-year-old postmenopausal woman with an ovarian cellular fibroma. Ultrasonography, computed tomography, and magnetic resonance imaging (MRI) revealed an 8 cm solid mass in the left adnexal area with minimal amount of ascites. On T2-weighted imaging (T2WI), the solid portion on the right side of the mass was mildly hyperintense, with the presence of several cystic components, while the smaller solid portion on the left side was hypointense. A diffusion-restricted site was also observed in the right solid portion of the mass. On dynamic contrast-enhanced MRI, the entire solid portion of the mass showed a faint and gradual enhancement pattern, suggesting a fibrous tumor. Since it could not be confidently diagnosed as an observable benign tumor, diagnostic laparoscopic surgery was performed to remove the mass, and following pathological examination of the tumor, a diagnosis of ovarian cellular fibroma was established. Microscopically, most areas of the tumor showed high cellularity, consistent with the diffusion-restricted site observed on MRI. However, some areas of normal density existed. In cases wherein a fibrous ovarian tumor exhibits diffusion restriction, cellular fibroma should be considered. This finding could have the potential to contribute to preoperative diagnosis and aid in the selection of treatment options.

**Keywords:** Ovary; Cellular fibroma; Ovarian tumor; Magnetic resonance imaging; Diffusion-weighted imaging; Laparoscopy; Pathology

Manuscript submitted May 20, 2024, accepted June 28, 2024  
Published online July 18, 2024

<sup>a</sup>Department of Obstetrics and Gynecology, Chibune General Hospital, Osaka 555-0034, Japan

<sup>b</sup>Department of Radiology, Chibune General Hospital, Osaka 555-0034, Japan

<sup>c</sup>Department of Radiology, Hyogo College of Medicine Hospital, Hyogo 663-8501, Japan

<sup>d</sup>Department of Pathology, Chibune General Hospital, Osaka 555-0034, Japan

<sup>e</sup>Corresponding Author: Yuka Sano, Department of Obstetrics and Gynecology, Chibune General Hospital, Osaka 555-0034, Japan.  
Email: yuka.sano.1210@gmail.com

doi: <https://doi.org/10.14740/jcgo981>

## Introduction

Ovarian cellular fibromas are relatively rare compared with the common benign ovarian fibromas [1, 2]. An ovarian fibroma with a high density of tumor cells and mild cellular atypia is referred to as a cellular fibroma. Cellular fibromas account for approximately 10% of ovarian fibromas and have uncertain malignant potential [3]. The magnetic resonance imaging (MRI) findings of this type of tumor are lacking in the literature. Thus, we present the radiological findings, particularly those of MRI, including diffusion-weighted imaging (DWI) and dynamic contrast-enhanced imaging (DCE), in a case of ovarian cellular fibroma.

## Case Report

### Investigations

A 60-year-old postmenopausal woman, gravida 2 para 1, was found to have a pelvic mass during a medical check-up. The patient had no symptoms or relevant medical history. There was no significant family history reported. The patient was referred to the Department of Obstetrics and Gynecology of our hospital wherein ultrasonography was performed. It revealed an echogenic mass with smooth, well-defined borders in the left adnexal area. Posterior acoustic shadowing was also observed. The mass exhibited hypo-vascularization on color Doppler study (Fig. 1). The right ovary appeared normal with minimal ascites present. Serum levels of tumor markers, such as CA19-9, CA125, and carcinoembryonic antigen (CEA), were within normal ranges while the serum level of estradiol (E2) was 16 pg/mL (normal range: < 39 pg/mL). Subsequent computed tomography (CT) revealed an 8 cm cystic and solid mass in the left ovary (Fig. 2). MRI of the lower abdomen was performed using a 3T MAGNETOM Skyra (Siemens Healthineers, Erlangen, Germany). The left ovarian solid mass with cystic components was well circumscribed and isointense compared with the skeletal muscle on T1-weighted imaging (T1WI) (Fig. 3a). On T2-weighted imaging (T2WI), the mass comprised a mildly hyperintense solid portion on the right side, which included several cystic components, and a smaller, hypointense, solid portion on the left side (Fig. 3b). On DWI with a b-value of 800 s/mm<sup>2</sup>, the larger solid portion on the right side of the

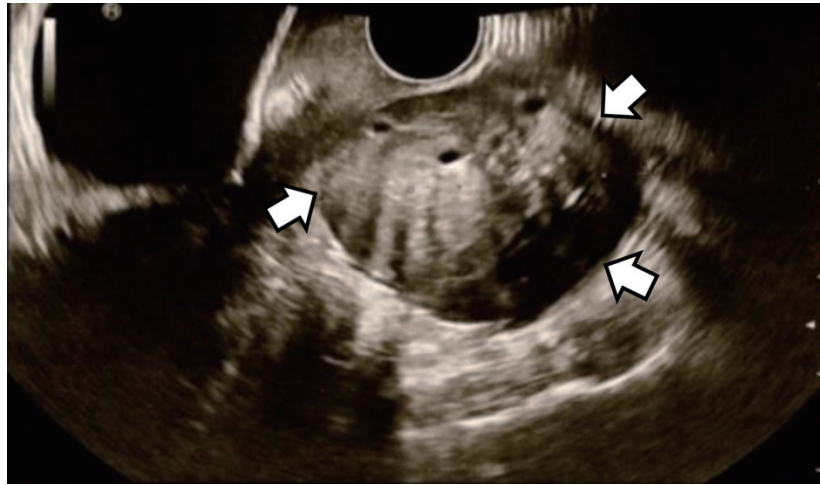


**Figure 1.** Transvaginal ultrasound image. In the left adnexal area, an echogenic mass with smooth, well-defined borders can be observed (arrows). Posterior acoustic shadowing is also observed.

mass showed hyperintensity. However, hypointensity was observed on the apparent diffusion coefficient (ADC) map. The left solid portion of the mass showed an absence of restriction (Fig. 3c, d). On DCE-MRI, compared with pre-contrast T1WI, the entire solid portion excluding cystic components of the mass showed a faint and gradual enhancement pattern, whereas the uterine myometrium showed relatively strong enhancement (Fig. 3e, f).

## Diagnosis

The patient was asymptomatic, having no relevant medical or family history, without evident findings, including tumor markers, of blood tests. Using ultrasound examination, a solid tumor with poor vascularity was observed. Although the MRI



**Figure 2.** Axial contrast-enhanced computed tomography. Uneven faint enhancement of the left ovarian tumor (arrows) can be observed.

findings suggested a tumor with abundant fibrous component, no definitive diagnosis of benign fibroma was made. Based on perspective of these, definitively distinguishing between benign and malignant entities was deemed impossible. Given the patient's strong preference to minimally invasive surgery, we decided to proceed with laparoscopic left adnexectomy and abdominal fluid aspiration.

## Treatment

During surgery, an 8 cm yellowish-white solid mass was identified on the left ovary, exhibiting torsion of approximately one rotation without necrotic appearance. The uterus and right ovary showed unremarkable findings. There were no findings of intraperitoneal dissemination (Fig. 4). Furthermore, there was a minimal accumulation of ascitic fluid, for which cytology revealed negative results. We performed laparoscopic left adnexectomy and retrieved the dissected specimen within a retrieval bag after extending the umbilical incision. The bag remained intact throughout the procedure, ensuring that no tumor spillage occurred within the peritoneal cavity.

Pathological examination of the entire excised mass revealed a solid mass with a yellowish-white wall. Microscopic examination revealed ovarian cortical stroma-like spindle-shaped tumor cells arranged in bundles that were proliferating in a fulfilling manner (Fig. 5a). Most areas of the mass showed hypercellularity. However, some areas of normal density were mixed (Fig. 5c). Mild-to-moderate nuclear atypia was also observed. The density of tumor cells was high, with 3.06 mitoses/2.4 mm<sup>2</sup> observed (Fig. 5b). There were no prominent findings of necrosis suggestive of torsion. Based on these findings, the final diagnosis was cellular fibroma.

## Follow-up and outcomes

There were no adverse or unanticipated events. Postoperative



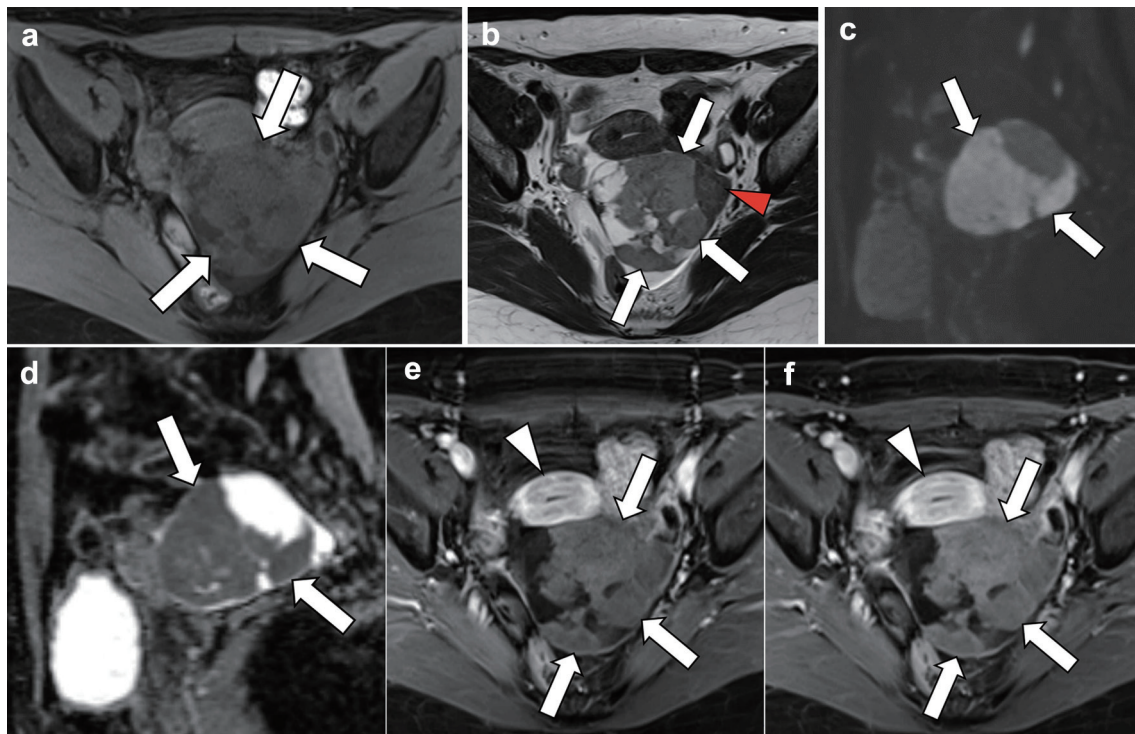


**Figure 3.** Magnetic resonance imaging. (a) T1-weighted axial section, (b) T2-weighted axial section, (c, d) diffusion-weighted sagittal images, and (e, f) dynamic contrast-enhanced axial images. On T2-weighted imaging, the left ovarian mass is mildly hyperintense in the larger right solid portion (b; arrows), with several cystic areas detected, and hypointense in the smaller left solid portion (arrowhead). On diffusion-weighted imaging, reduced diffusion is observed in the solid portion of the mass (c, d; arrows), which is pathologically proven to be a cellular fibroma component with hypercellularity. On dynamic contrast-enhanced imaging, compared with pre-contrast T1WI, the entire solid portion excluding cystic components of the mass shows a faint and gradual enhancement pattern (e, f; arrows), corresponding to a tumor with abundant fibrous components pathologically proven, whereas the uterine myometrium shows relatively strong enhancement (arrowheads).

recovery was favorable, and the patient was discharged from our hospital 5 days after surgery. After discharge, the patient underwent outpatient follow-up visits. The patient has not experienced any recurrence within 1 year since the surgery.

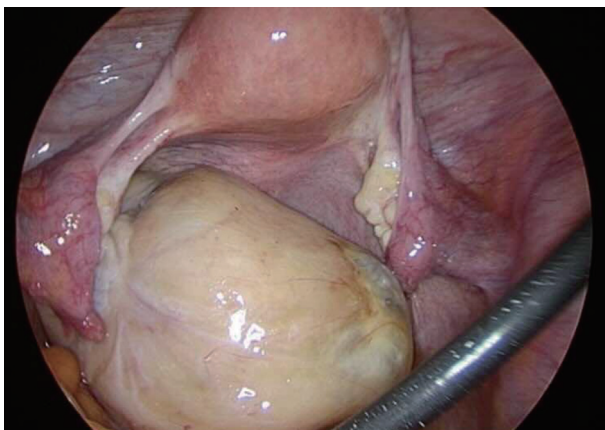


**Figure 4.** Laparoscopic findings. A yellowish-white solid mass is detected on the left ovary, showing torsion of approximately one rotation without any signs of necrosis. The uterus and right ovary appeared within normal range. No evidence of intraperitoneal dissemination is observed. There is a small amount of ascitic fluid accumulation.

## Discussion

Ovarian fibroma is the most common benign tumor of the ovarian stroma, accounting for 4% of all ovarian neoplasms [1]. Ovarian fibromas can occur at any age, and approximately 10% of ovarian fibromatous tumors exhibit hypercellularity, increased mitotic activity, and mild-to-moderate nuclear atypia, which are subsequently termed “cellular fibromas” [2]. Cellular fibromas are tumors with uncertain malignant potential, which may recur or be associated with peritoneal implants. The degree of mitotic activity is the primary parameter used to differentiate cellular fibromas from fibrosarcomas [2, 3].

Although cases of ovarian cellular fibroma have been reported in the literature, detailed imaging findings, particularly MRI, are lacking. Adad et al described a case of ovarian cellular fibroma with CT findings, indicating a contrast-enhanced solid area in the cyst wall. However, MRI findings were not reported [3]. Shinagare et al reported MRI features of solid ovarian tumors, including two cases of cellular fibroma. However, only T2WI was presented [4]. In a review of solid ovarian tumors by Mukuda et al, MRI findings of cellular fibromas, including T2WI, DWI, and DCE-T1WI, were presented, but only the images were mentioned; pathological findings and clinical course were not presented [5]. This is the first case

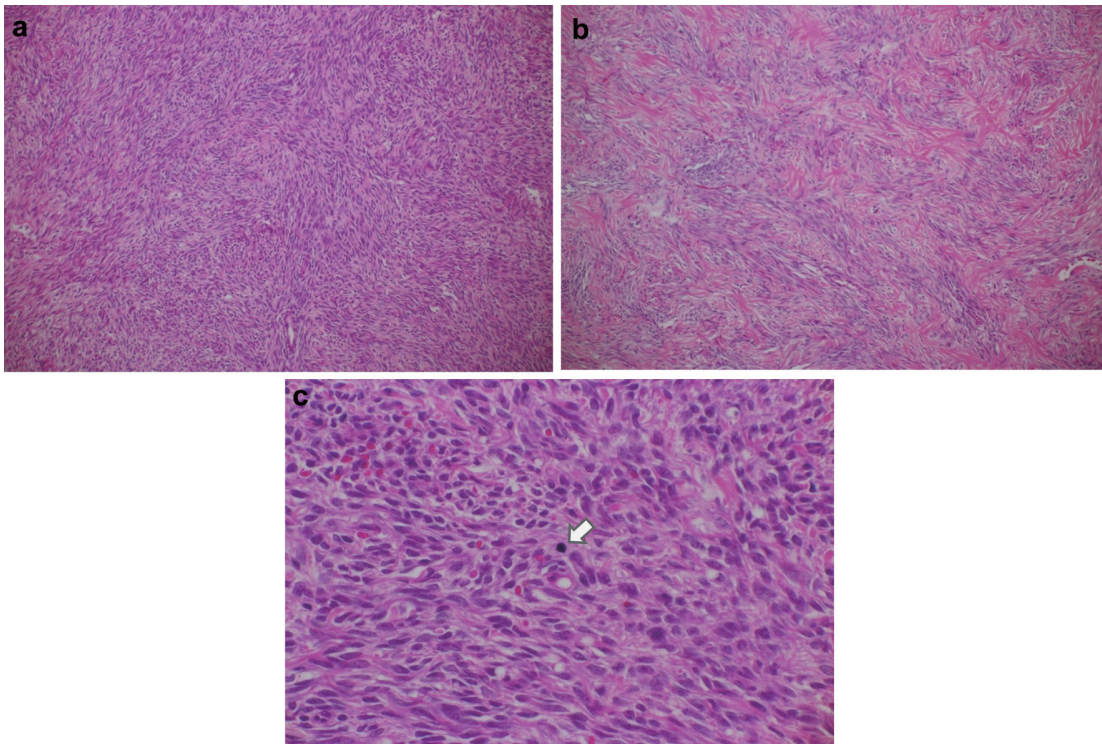


**Figure 5.** Histologic features of the ovarian tumor. (a) Cellular fibroma (hematoxylin and eosin, original magnification  $\times 100$ ). This pathological specimen shows abundant spindle-shaped cells and fibrocollagenous stroma. Spindle-shaped cells occupy a relatively large area, and mitotic figures are widely found compared with the ordinary fibroma. (b) Ordinary fibroma (hematoxylin and eosin, original magnification  $\times 100$ ). The density of spindle-shaped cells is lower than in (a). (c) Cellular fibroma containing cells undergoing mitosis (arrow) (hematoxylin and eosin, original magnification  $\times 400$ ). Arranged spindle-shaped cells can be seen as well as mitotic figures (average 3.06 mitoses/2.4 mm<sup>2</sup>). Overall, no prominent findings indicative of extensive necrosis.

report to present the correlation between MRI and pathological findings of this rare tumor.

In the present case, the mass was isointense compared with the skeletal muscle on T1WI; while on T2WI, the right solid portion of the mass, constituting the majority of the tumor, was mildly hyperintense and the left solid portion was hypointense (Fig. 3a, b). On DWI, the right solid portion showed hyperintensity, which was pathologically proven to be a cellular fibroma component with hypercellularity (Figs. 3c, 5a). In contrast, the left solid portion, which showed an absence of restriction, was proven to be a regular fibroma component (Figs. 3c, 5b). DWI generally reflects the cellular density of a lesion. Thus, the current DWI findings are consistent with the result of the histological examination that most areas of the mass showed hypercellularity and some areas of normal density were mixed.

Kitajima et al reported that ovarian fibromas typically exhibit a low signal intensity on T2WI and weak enhancement with contrast material [1]. In the present case, the smaller left solid portion of the mass exhibited low signal intensity on T2WI while the diffusion-restricted solid portion on the right side of the mass exhibited a weak enhancement. The entire solid portion of the mass, regardless of the area, showed a faint and gradual enhancement pattern on DCE-MRI, suggesting a tumor with abundant fibrous components. Torsion of the current affected ovary was identified during surgery. The torsed ovary is characterized by disrupted blood flow, which is seen

as abnormal enhancement after intravenous contrast agent administration. Heterogeneous minimal or absent enhancement indicates the evolution of ovarian torsion from ischemia to infarction [6]. However, the torsion of approximately one rotation was without necrotic appearance without observing pathological findings of necrosis or infarction. Thus, in this case, torsion might be considered to have little effect on the contrast effect of the tumor. Based on these findings, without those from DWI, the tumor of the present case could have been presumed to be a fibrous tumor containing ordinary fibroma components, thus highlighting the difficulty in distinguishing between benign and malignant tumors.

Regarding fibrous tumors, differentiating fibrosarcomas from other tumors is important. Although no detailed studies on the imaging findings of this malignant tumor exist in the literature, previously published case reports indicate that fibrosarcomas tend to show abundant vascularity on CT or ultrasound [7, 8]. Fibrosarcoma could be ruled out in the current case as only faint contrast enhancement was observed by DCE-MRI.

Although the MRI findings suggested the possibility of borderline malignant tumor, including granulosa cell tumor, the tools of routine clinical practice, including imaging and serum tumor marker levels, were unable to distinguish benign from malignant disease in the present case. Laparoscopic surgery, and subsequent histological analysis of the mass, enabled an accurate diagnosis to be made in this particular uncertain



clinical situation [9]. In this case, preoperative diagnosis was inconclusive; retrospective analysis was undertaken following the pathological findings. Although this case serves as a single example, we aspire to gather analogous cases in the future and conduct a thorough analysis of their characteristics.

### Learning points

Various MRI findings of the rare tumor of the present case, the ovarian cellular fibroma, well correlated with the pathology. The preoperative diagnosis of this disease may be overlooked owing to its rarity. However, a combination of atypical findings on DWI and findings typical of a fibrous lesion on DCE may be the key to considering this rare tumor as a differential diagnosis in cases involving ovarian masses. We recommend including these imaging techniques for cases of relatively large solid ovarian tumors. These techniques could have the potential to contribute to preoperative diagnosis and aid in the selection of treatment options.

### Acknowledgments

The authors thank the Department of Obstetrics and Gynecology and Radiology at Chibune General Hospital.

### Financial Disclosure

This study did not receive any specific grant from funding agencies in the public, commercial, or not-for-profit sectors.

### Conflict of Interest

None to declare.

### Informed Consent

The patient of the present case provided written informed consent. We confirm the ethical approval of the case report.

### Author Contributions

Yuka Sano, Tetsuo Maeda, Takahiro Watanabe, and Shigeki Yoshida observed the patient and performed medical treatment. Yuka Sano, Tetsuo Maeda, Takahiro Watanabe, Mieko Inagaki, and Shigeki Yoshida drafted, reviewed, edited the manuscript. All authors have approved the final article for journal publication.

### Data Availability

Date sharing is not applicable to this article as no new data were created or analyzed in this study.

### Abbreviations

ADC: apparent diffusion coefficient; CT: computed tomography; DCE: dynamic contrast-enhanced imaging; DWI: diffusion-weighted imaging; MRI: magnetic resonance imaging; T1WI: T1-weighted imaging; T2WI: T2-weighted imaging

### References

1. Kitajima K, Kaji Y, Sugimura K. Usual and unusual MRI findings of ovarian fibroma: correlation with pathologic findings. *Magn Reson Med Sci*. 2008;7(1):43-48. [doi](#) [pubmed](#)
2. Prat J, Scully RE. Cellular fibromas and fibrosarcomas of the ovary: a comparative clinicopathologic analysis of seventeen cases. *Cancer*. 1981;47(11):2663-2670. [doi](#) [pubmed](#)
3. Adad SJ, Laterza VL, Dos Santos CD, Ladeia AA, Saldanha JC, da Silva CS, LR ES, et al. Cellular fibroma of the ovary with multiloculated macroscopic characteristics: case report. *Case Rep Med*. 2012;2012:283948. [doi](#) [pubmed](#) [pmc](#)
4. Shinagare AB, Meylaerts LJ, Laury AR, Morteale KJ. MRI features of ovarian fibroma and fibrothecoma with histopathologic correlation. *AJR Am J Roentgenol*. 2012;198(3):W296-303. [doi](#) [pubmed](#)
5. Mukuda N, Ishibashi M, Murakami A, Fukunaga T, Fujii S. Ovarian solid tumors: MR imaging features with radiologic-pathologic correlation. *Jpn J Radiol*. 2020;38(8):719-730. [doi](#) [pubmed](#)
6. Duigenan S, Oliva E, Lee SI. Ovarian torsion: diagnostic features on CT and MRI with pathologic correlation. *AJR Am J Roentgenol*. 2012;198(2):W122-131. [doi](#) [pubmed](#)
7. Miura M, Suzuki S, Shibata K, Kajiyama H, Kikkawa F. Estrogen producing ovarian fibrosarcoma: A case report. *Nagoya J Med Sci*. 2019;81(1):171-176. [doi](#) [pubmed](#) [pmc](#)
8. Sun TT, Cheng NH, Cao DY, Peng P. Ovarian fibrosarcoma: A single-institution experience and a review of the literature. *J Ovarian Res*. 2020;13(1):142. [doi](#) [pubmed](#) [pmc](#)
9. Son CE, Choi JS, Lee JH, Jeon SW, Hong JH, Bae JW. Laparoscopic surgical management and clinical characteristics of ovarian fibromas. *JSLs*. 2011;15(1):16-20. [doi](#) [pubmed](#) [pmc](#)